J. Fluid Mech. (2007), *vol.* 576, *pp.* 475–490.
doi:10.1017/S0022112007004806 Printed in the United Kingdom

The effect of disturbances on the flows under a sluice gate and past an inclined plate

B. J. BINDER[1] AND J.-M. VANDEN-BROECK[2]

[1]School of Mathematical Sciences, University of Adelaide, Adelaide 5005, South Australia
[2]School of Mathematics, University of East Anglia, Norwich NR4 7TJ, UK

(Received 8 March 2006 and in revised form 7 November 2006)

Free surface potential flows past disturbances in a channel are considered. Three different types of disturbance are studied: (i) a submerged obstacle on the bottom of a channel; (ii) a pressure distribution on the free surface; and (iii) an obstruction in the free surface (e.g. a sluice gate or a flat plate). Surface tension is neglected, but gravity is included in the dynamic boundary condition. Fully nonlinear solutions are computed by boundary integral equation methods. In addition, weakly nonlinear solutions are derived. New solutions are found when several disturbances are present simultaneously. They are discovered through the weakly nonlinear analysis and confirmed by numerical computations for the fully nonlinear problem.

1. Introduction

We consider nonlinear two-dimensional potential free-surface flows past disturbances in a channel. As reviewed below, many results have been obtained for flows past a single disturbance. The focus of this paper is on flows past multiple disturbances. This enables us to generate new families of solutions which do not have an equivalent when there is only one disturbance. In particular, it was found in Binder & Vanden-Broeck (2005) that there are no steady potential flows past a sluice gate or wavy flows past a flat plate which satisfy the radiation condition (this condition which requires that there is no energy coming from infinity, implies that the flow is not wavy upstream). In this paper, it is shown that such solutions can be obtained by introducing a second disturbance in the flow. The disturbances can be submerged or on the free surface. We consider three types of disturbance: (i) an obstacle on the bottom of a channel (e.g. a triangle); (ii) a pressure distribution on the free surface (e.g. a ship); and (iii) an obstruction in the free surface (e.g. a sluice gate or a flat plate).

As $x^* \to \infty$, the flow is assumed to approach a uniform stream with constant velocity U and constant depth H, (figure 1*a*). We define the dimensionless downstream Froude number as

$$F = \frac{U}{(gH)^{1/2}}. \tag{1.1}$$

Here, g is the acceleration due to gravity. As $x^* \to -\infty$, the flow can be uniform or be characterized by a train of waves of constant amplitude. When it is uniform, we introduce an (additional) upstream Froude number

$$F^* = \frac{V}{(gD)^{1/2}}, \tag{1.2}$$

where V and D are the uniform velocity and uniform depth as $x^* \to -\infty$.

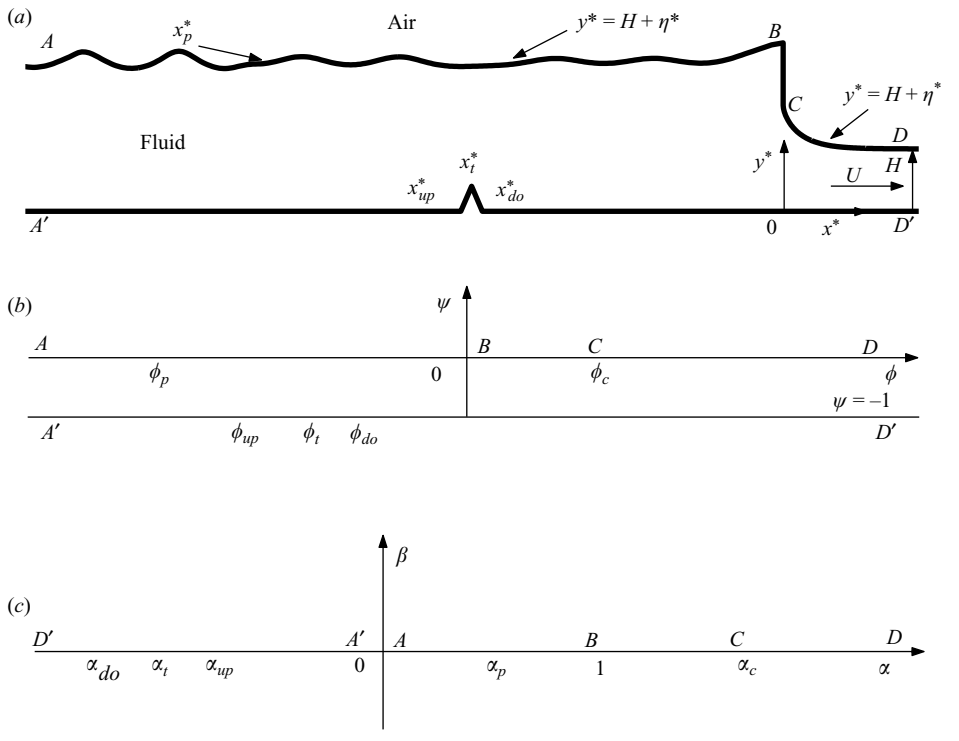

FIGURE 1. (*a*) Sketch of flow in physical coordinates (x^*, y^*). The three types of disturbance are illustrated. The first is a submerged triangle at the bottom of the channel. The second is a distribution of pressure centred at x_p^* (only the centre is shown in the sketch). The third is a gate BC in the free surface. (*b*) Sketch of flow in the plane of the complex potential (f-plane). (*c*) Sketch of flow in the lower half-plane (ζ-plane).

Free-surface flows past a single disturbance have been studied by many previous investigators. For example, flows past the first two types of disturbance (submerged disturbances and pressure distributions) were investigated by Lamb (1945), Forbes (1981), Forbes & Schwartz (1982), Vanden-Broeck (1987), Forbes (1988), Dias & Vanden-Broeck (1989), Asavanant & Vanden-Broeck (1994), Shen (1995) and others. Three different types of flow were found. The first type is characterized by uniform streams both far upstream and far downstream (i.e. as $x^* \to \pm\infty$) with $F = F^* > 1$. The second type has a uniform stream as $x^* \to \infty$ with $F < 1$ and a train of waves as $x^* \to -\infty$. The third type is characterized by uniform flows as $x^* \to \pm\infty$ with $F > 1$ and $F^* < 1$.

Dias & Vanden-Broeck (2002) identified a fourth type of flow characterized by a uniform stream with $F > 1$ as $x^* \to \infty$ and by a train of waves as $x^* \to -\infty$. These flows do not satisfy the radiation condition if the flow is oriented as in figure 1(*a*). Therefore, the physical relevance of these new flows appears to be limited in the case of one obstacle.

Many calculations were also performed for the third type of disturbance (obstruction in the free surface). For free-surface flows under sluice gates and past plates (see for example Binnie 1952; Benjamin 1956; Frangmeier & Strelkoff 1968; Larock 1969; Chung 1972; Vanden-Broeck & Keller 1989; Asavanant & Vanden-Broeck 1996; Vanden-Broeck 1996; Binder & Vanden-Broeck 2005). The flow under a sluice gate (with the flow orientation of figure 1*a*) is defined by uniform streams

as $x^* \to \pm\infty$ with $F > 1$ and $F^* < 1$. Experiments show that eddying motion in front of the gate and wave generation by upstream conditions may occur (see Benjamin 1956). However, such effects are neglected in most investigations and steady potential solutions are sought. Unfortunately, Vanden-Broeck (1996) and Binder & Vanden-Broeck (2005) showed that there are no such flows. The only possible 'solutions' for flows under a sluice gate are characterized by a uniform stream with $F > 1$ as $x^* \to \infty$ and a train of waves as $x^* \to -\infty$. These 'solutions' are similar to the fourth type of solutions past a submerged disturbance calculated by Dias & Vanden-Broeck (2002) in the sense that they do not satisfy the radiation condition.

Binder & Vanden-Broeck (2005) also showed that there are no flows past a flat plate with a uniform stream with $F < 1$ as $x^* \to \infty$ and a train of waves as $x^* \to -\infty$. Only solutions with trains of waves as $x^* \to \pm\infty$ can be calculated. Again these solutions cannot satisfy the radiation condition.

Dias & Vanden-Broeck (2004) examined further the flows of the fourth type past an obstacle. They consider flows past two obstacles and obtain new solutions which are characterized by a train of waves trapped between the two obstacles. These solutions satisfy the radiation condition. The flows of the fourth type were shown to describe locally the flow over one of the obstacles when the distance between the obstacles is large. This work was extended by Binder, Dias & Vanden-Broeck (2005).

In this paper, we examine further the two solutions of Binder & Vanden-Broeck (2005) which do not satisfy the radiation condition (i.e. the flow under a sluice gate and the wavy flow past a flat plate). The results of Dias & Vanden-Broeck (2004) suggest that placing a second disturbance in front of the gate or the plate might generate physical flows which satisfy the radiation condition. The idea is to trap the waves (which appear as $x^* \to -\infty$ in the solutions of Binder & Vanden-Broeck 2005) between the two disturbances so that the flow becomes uniform as $x^* \to -\infty$. The radiation condition is then satisfied. In this paper, we provide conclusive analytical and numerical evidence that such solutions exist. This provides a physical interpretation of the solutions of Binder & Vanden-Broeck (2005), which do not satisfy the radiation condition: they describe locally the flow near the sluice gate or plate when the second obstruction is far away. In addition, we compute new families of solutions.

The numerical solutions are obtained via a boundary-integral-equation formulation of the fully nonlinear problem. The analytical results are based on a weakly nonlinear theory. Both approaches are described in § 2.

When presenting the results, we shall use the following terminology. The flow of figure 1(*a*) is called supercritical, if it is uniform both far upstream and far downstream (i.e. as $x^* \to \pm\infty$ with $F = F^* > 1$). It is called subcritical if it is uniform as $x^* \to \infty$ with $F < 1$ and characterized by a train of waves as $x^* \to -\infty$. If the flow is uniform as $x^* \to \pm\infty$ with $F > 1$ and $F^* < 1$, the flow is called critical. Finally, it is called a generalized critical flow if the flow is uniform with $F > 1$ as $x^* \to \infty$ and characterized by a train of waves as $x^* \to -\infty$.

2. Formulation

We consider the steady two-dimensional irrotational flow of an inviscid and incompressible fluid in a channel. The fluid has constant density ρ. We define Cartesian coordinates (x^*, y^*) with the x^*-axis on the horizontal bottom and the y^*-axis directed vertically upwards, (see figure 1*a*). Gravity is acting in the negative y^*-direction and surface tension is neglected. As $x^* \to \infty$, the flow approaches a uniform stream with constant velocity U and constant depth H.

We denote the equation of the free surface by $y^* = H + \eta^*(x^*)$ where $\eta^*(x^*)$ is the elevation of the free surface on top of the level $y^* = H$.

We assume that the flow is perturbed by disturbances. The first type is an obstacle on the channel bottom. In this paper, we consider isosceles triangles with angle $180^\circ - 2\sigma_t$ at their apexes. Qualitatively similar results could be obtained for other shapes. We denote the position of the triangle's apex by x_t^* and the position of the corners on the bottom by x_{do}^* and x_{up}^*, (see figure 1*a*). Here, *do* and *up* refers to downstream and upstream, respectively. The triangle has height h^*. The equation for the shape of the channel bottom is denoted by $y^* = \sigma^*(x^*)$.

The second type is a pressure distribution $P^*(x^*)$ with bounded support. This could model the effect of the wind or a ship for example. In the sketch of figure 1(*a*), there is a distribution of pressure with centre at x_p^* on the upstream free surface AB. The third type is an obstruction in the free surface. An example is a sluice gate or a surfboard, length L^*, inclined at angle σ_c to the horizontal. In figure 1(*a*), there are two free surfaces AB and CD with a vertical sluice gate BC.

Two theories are used in this paper to solve the flow problem in figure 1(*a*). The first is a nonlinear numerical theory based on boundary-equation methods. The second is an analytical weakly nonlinear theory using the Korteweg–de Vries equation (KdV) and forced Korteweg–de Vries equations (fKdV). The numerical method used to compute nonlinear solutions is described in the next subsection.

2.1. *Boundary-integral equation*

The numerical procedure is derived as a combination of the methods used by Binder *et al.* (2005) to compute flows past submerged obstacles and by Vanden-Broeck (1996) and Binder & Vanden-Broeck (2005) to compute flows under sluice gates or past flat plates. Some of the details are repeated for completeness and further details can be found in these papers.

We define dimensionless variables by taking H as the reference length and U as the reference velocity. Thus, we define the dimensionless quantities $(x, y, \eta, \sigma, L, h) = (x^*, y^*, \eta^*, \sigma^*, L^*, h^*)/H$ and $(u, v) = (u^*, v^*)/U$. Here, u^* and v^* are the dimensional horizontal and vertical components of the velocity. We also define the dimensionless pressure $P(x) = P^*(x^*)/\rho g H$.

The dynamic boundary condition, on the two free surfaces AB and CD, then takes the form

$$\frac{1}{2}(u^2 + v^2) + \frac{1}{F^2}(P + y) = \frac{1}{2} + \frac{1}{F^2} \quad \text{on} \quad y = 1 + \eta. \tag{2.1}$$

We introduce the complex potential function, $f = \phi + \mathrm{i}\psi$ and the complex velocity, $w = \mathrm{d}f/\mathrm{d}z = u - \mathrm{i}v$. Without loss of generality, we choose $\psi = 0$ on the streamline $ABCD$. It follows that $\psi = -1$ on the channel bottom streamline $A'D'$. We also choose $\phi = 0$ and $x = 0$ at the point B on the streamline $ABCD$. We denote by $\phi = \phi_c$ the value of ϕ at the point C where the downstream free surface separates from the gate. Similarly, we denote the values of ϕ at the corners of the triangle by ϕ_{up}, ϕ_{do} and ϕ_t. In the complex potential plane, the fluid is in the strip $-1 < \psi < 0$ and $-\infty < \phi < \infty$ (see figure 1*b*).

We then map the strip of figure 1(*b*) onto the lower half of the ζ-plane by the transformation

$$\zeta = \alpha + \mathrm{i}\beta = \exp(\pi f). \tag{2.2}$$

The flow in the ζ-plane is shown in figure 1(*c*), where $\alpha_c = \exp(\pi\phi_c)$, $\alpha_p = \exp(\pi\phi_p)$, $\alpha_{up} = -\exp(\pi\phi_{up})$, $\alpha_t = -\exp(\pi\phi_t)$ and $\alpha_{do} = -\exp(\pi\phi_{do})$. The objective now is to derive

integral equation relations that only involve unknown quantities on the free surface, subject to the kinematic boundary conditions on the free surface, the gate and the bottom of the channel.

We first define the function $\tau - \mathrm{i}\theta$ by

$$w = u - \mathrm{i}v = \exp(\tau - \mathrm{i}\theta). \tag{2.3}$$

Following Binder *et al.* (2005) and Binder & Vanden-Broeck (2005), we obtain the following relation for τ in terms of the unknown function θ on the free surfaces AB and CD

$$\tau(\phi) = -\frac{\sigma_t}{\pi}\ln\frac{(\alpha_t - \exp(\pi\phi))^2}{|(\alpha_{up} - \exp(\pi\phi))(\alpha_{do} - \exp(\pi\phi))|} - \frac{\sigma_c}{\pi}\ln\frac{|\alpha_c - \exp(\pi\phi)|}{|1 - \exp(\pi\phi)|} + \int_{-\infty}^{0}\frac{\theta(\phi_0)\exp(\pi\phi_0)}{\exp(\pi\phi_0) - \exp(\pi\phi)}\,\mathrm{d}\phi_0 + \int_{\phi_c}^{\infty}\frac{\theta(\phi_0)\exp(\pi\phi_0)}{\exp(\pi\phi_0) - \exp(\pi\phi)}\,\mathrm{d}\phi_0. \tag{2.4}$$

Parametric relations for the shape of the upstream free surface, AB, in terms of $\tau(\phi)$ and $\theta(\phi)$ are

$$x(\phi) = \int_0^{\phi}\exp(-\tau\phi_0)\cos\theta(\phi_0)\,\mathrm{d}\phi_0 \quad \text{for} \quad -\infty < \phi < 0 \tag{2.5}$$

and

$$y(\phi) = y(0) + \int_0^{\phi}\exp(-\tau\phi_0)\sin\theta(\phi_0)\,\mathrm{d}\phi_0 \quad \text{for} \quad -\infty < \phi < 0. \tag{2.6}$$

Those on the downstream free surface CD are

$$x(\phi) = x(\phi_c) + \int_{\phi_c}^{\phi}\exp(-\tau\phi_0)\cos\theta(\phi_0)\,\mathrm{d}\phi_0 \quad \text{for} \quad \phi_c < \phi < \infty \tag{2.7}$$

and

$$y(\phi) = 1 + \int_{\infty}^{\phi}\exp(-\tau\phi_0)\sin\theta(\phi_0)\,\mathrm{d}\phi_0 \quad \text{for} \quad \phi_c < \phi < \infty. \tag{2.8}$$

The quantities $y(0)$ and $x(\phi_c)$ in (2.6) and (2.7) can be evaluated as follows. If the free surface separates tangentially at B then

$$y(0) = \left(1 + \tfrac{1}{2}F^2\right)\gamma,$$

where the value $\gamma < 1$ fixes the position of the separation point. If B is a stagnation point, then $\gamma = 1$. For a vertical gate $x(\phi_c) = 0$ and for a inclined gate $x(\phi_c) = (y(0) - y(\phi_c))/\tan\sigma_c$.

As we shall see in § 2.2, the weakly nonlinear theory approximates the pressure P by a delta function. In the nonlinear computations we choose

$$P(x) = A\frac{\beta}{\sqrt{\pi}}\exp(-\beta^2(x - x_p)^2), \tag{2.9}$$

where A and β are constants. It can be shown that

$$P(x) \to A\delta(x - x_p) \quad \text{as} \quad \beta \to \infty. \tag{2.10}$$

The fact that $P(x)$ is close to a delta function for β large, will be convenient when comparing nonlinear results with weakly nonlinear results. Equations (2.1), (2.4), (2.6) and (2.8) define a nonlinear integral equation for the unknown function $\theta(\phi)$ on the free surfaces $-\infty < \phi < 0$ and $\phi > \phi_c$.

This integral equation is solved numerically by following the numerical procedures outlined in Binder *et al.* (2005) and Binder & Vanden-Broeck (2005). Other equations for the length of the gate, L, and height of triangle, h, can also be found in these papers.

2.2. *Weakly nonlinear theory*

The determination of the number of independent parameters required to obtain a unique solution to a free-surface problem is often delicate and counter intuitive. There are two ways to find them. The first is by careful numerical experimentation (fixing too many or too few parameters fails to yield convergence); the second is to perform a weakly nonlinear analysis in the phase plane. This second approach has the advantage of allowing a systematic determination of all the possible solutions (within the range of validity of the weakly nonlinear analysis). In all the examples presented in this paper, we checked that both approaches lead to the same number of independent parameters.

Shen (1995), Dias & Vanden-Broeck (2002), Binder *et al.* (2005) and others derived a forced Korteweg–de Vries equation (fKdV equation) to model the flow past disturbances of the first two types (i.e. an obstacle at the bottom of the channel and a distribution of pressure). They showed that the forcing can be approximated by a jump in η_x. More precisely, they showed that the flow past an isosceles triangle of height h characterized by $\sigma_t = 45^\circ$ and centred at $x = x_t$ can be modelled by

$$\eta_{xx} + \tfrac{9}{2}\eta^2 - 6(F-1)\eta = 0 \quad \text{for} \quad x \neq x_t, \tag{2.11}$$

with the vertical jump condition

$$\eta_x(x_t^+) - \eta_x(x_t^-) = -3h^2. \tag{2.12}$$

Similarly, they showed that the flow past the distribution of pressure (2.9) (with β large) can be modelled by

$$\eta_{xx} + \tfrac{9}{2}\eta^2 - 6(F-1)\eta = 0 \quad \text{for} \quad x \neq x_p, \tag{2.13}$$

with the vertical jump condition

$$\eta_x(x_p^+) - \eta_x(x_p^-) = -3A. \tag{2.14}$$

These approximations are valid for small disturbances and F close to 1.

We define the jumps due to a submerged triangle and pressure distribution as

$$j_t = -3h^2, \qquad j_p = -3A, \tag{2.15}$$

respectively. These relations imply that a triangle and a distribution of pressure satisfying

$$h^2 = A, \tag{2.16}$$

produce the same weakly nonlinear solution.

Binder & Vanden-Broeck (2005) derived corresponding weakly nonlinear solutions for flows past a sluice gate or surfboard. They showed that the flow is described on the free surfaces AB and CD of figure 1(a) by the KdV equation

$$\eta_{xx} + \tfrac{9}{2}\eta^2 - 6(F-1)\eta = 0, \tag{2.17}$$

with the conditions

$$\eta^B - \eta^C = L\sin\sigma_c, \tag{2.18}$$

$$\eta_x^B = \eta_x^C = -\tan\sigma_c. \tag{2.19}$$

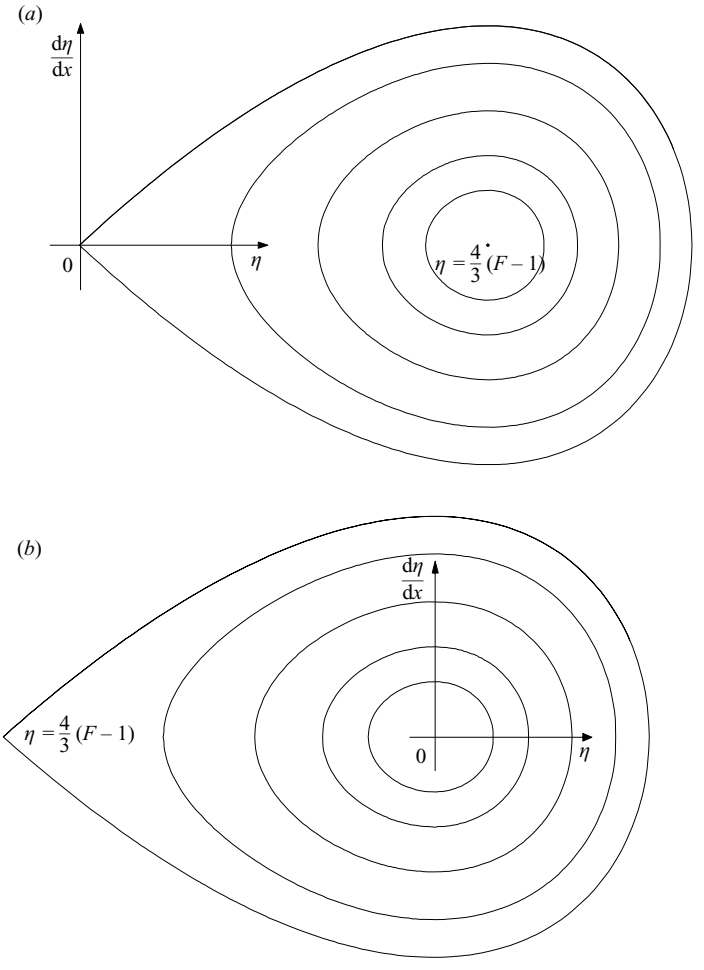

FIGURE 2. Weakly nonlinear phase portraits, $\mathrm{d}\eta/\mathrm{d}x$ versus η. (*a*) Supercritical flow, $F > 1$. There is a saddle point at $\eta = 0$, $\eta_x = 0$ and a centre at $\eta = 4/3(F-1)$, $\eta_x = 0$. (*b*) Subcritical flow, $F < 1$. There is a saddle point at $\eta = 4/3(F-1)$, $\eta_x = 0$ and a centre at $\eta = 0$, $\eta_x = 0$.

Here, the superscripts B and C refer to the points B and C in figure 1(*a*) and L is the length of the plate. Since $\eta_x^B = \eta_x^C$, (2.18) and (2.19) imply that the gate is represented in the phase plane by a horizontal segment of length $L \sin\sigma_c$. Following Binder & Vanden-Broeck (2005), we refer to that segment as a horizontal jump.

The free-surface flows considered in this paper involve multiple disturbances. The weakly nonlinear theory is obtained by combining the analysis for single disturbances developed by Dias & Vanden-Broeck (2002) (submerged disturbances) and by Binder & Vanden-Broeck (2005) (sluice gates). To construct weakly nonlinear solutions for flows past multiple disturbances we must combine the trajectories of the phase plane of figure 2 with both vertical jumps (submerged objects) and horizontal jumps (sluice gates or plates). Such analysis is performed in the next sections for supercritical, subcritical, (waveless) critical and generalized critical flow.

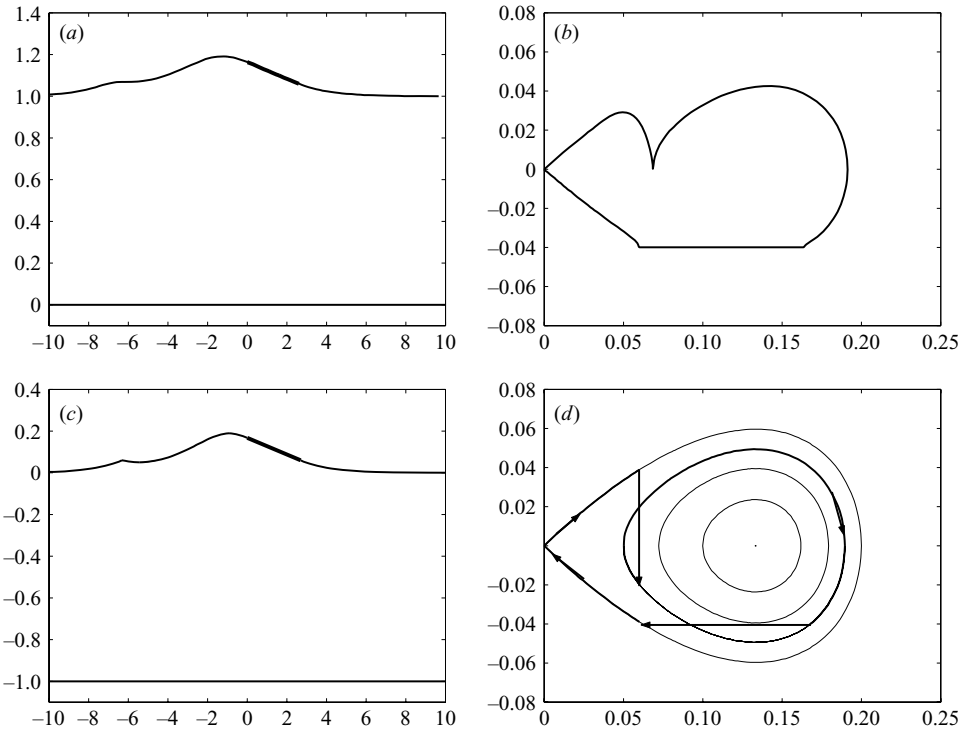

FIGURE 3. Supercritical flow past a pressure distribution and an inclined plate for given values of $F = 1.10$, $A = 0.02$ and $\sigma_c = 2.30°$. (*a*) Fully nonlinear free-surface profile for $\gamma = 0.72$, $L = 2.61$ and $x_p = -6.77$. (*b*) Values of $\mathrm{d}y/\mathrm{d}x = \tan(\theta)$ versus $y - 1 = \eta$, showing the fully nonlinear phase trajectories for (*a*). (*c*) Weakly nonlinear profile for $\gamma = 0.73$, $L = 2.70$ and $x_p = -6.32$. (*d*) Weakly nonlinear phase portrait for (*c*), $\mathrm{d}\eta/\mathrm{d}x$ versus η.

3. Results

3.1. *Supercritical flow past a pressure distribution and an inclined plate*

The main purpose of this paper is to construct weakly nonlinear and nonlinear solutions for subcritical flow past a plate and for critical flow under a sluice gate that satisfy the radiation condition. To complement these solutions we include here (see figure 3) weakly nonlinear and nonlinear solutions for supercritical flow past a pressure distribution and an inclined surfboard.

Supercritical flows are characterized by $F = F^* > 1$ and no waves as $x \to \pm\infty$. Figure 3(*a*) is a typical nonlinear free-surface profile for $F = 1.10$, $A = 0.02$, $\sigma_c = 2.30°$, $L = 2.61$, $\gamma = 0.72$ and $x_p = -6.77$. We now derive an analytical weakly nonlinear profile, (figure 3*c*) to compare with the our nonlinear computed profile (figure 3*a*). It is obtained by combining the phase plane of figure 2(*a*) with a vertical jump (modelling the pressure distribution) and a horizontal jump (modelling the plate). For example, in figure 3(*d*), we start at the origin in the phase plane moving along the solitary wave orbit in a clockwise direction until we come to the first disturbance (pressure distribution). There is then a vertical jump, given by (2.15), onto an inner periodic orbit in the phase plane. We then continue to move along this inner periodic orbit in a clockwise direction until we come to the second disturbance (inclined plate). There is then a horizontal jump, given by (2.18) and (2.19), onto the solitary wave orbit. We then continue to move along the solitary wave orbit until we return to the origin in

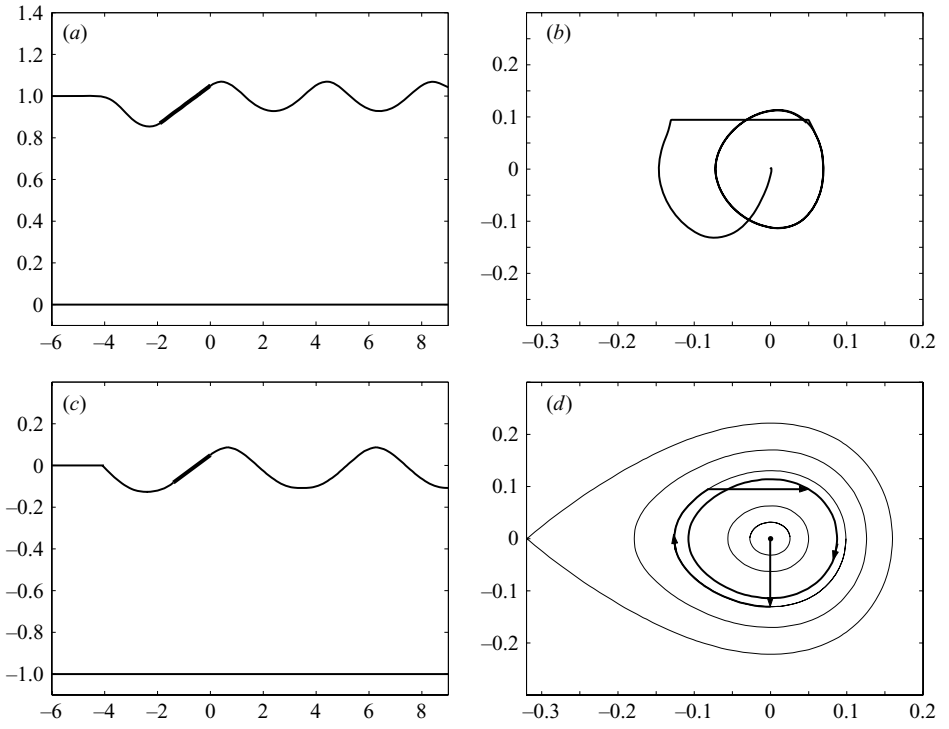

FIGURE 4. Subcritical flow past a pressure distribution and an inclined plate for given values of $F = 0.76$, $\gamma = 0.81$, $A = 0.04$ and $\sigma_c = -5.4°$. (*a*) Fully nonlinear free-surface profile for the values, $L = 1.92$ and $x_p = -3.60$. (*b*) Values of $\mathrm{d}y/\mathrm{d}x = \tan(\theta)$ versus $y - 1 = \eta$, showing the fully nonlinear phase trajectories for (*a*). (*c*) Weakly nonlinear profile for the values $L = 1.41$ and $x_p = -4.03$. (*d*) Weakly nonlinear phase portrait for (*c*), $\mathrm{d}\eta/\mathrm{d}x$ versus η.

the phase plane. The corresponding weakly nonlinear free-surface profile is shown in figure 3(*c*). The parameters for this weakly nonlinear solution are $F = 1.10$, $A = 0.02$, $\sigma_c = 2.30°$, $L = 2.70$, $\gamma = 0.73$ and $x_p = -6.32$. The weakly nonlinear and nonlinear solutions are qualitatively similar. In particular, the weakly nonlinear portrait of figure 3(*d*) is close to the curves of figure 3(*b*) where we plot nonlinear values of $\mathrm{d}y/\mathrm{d}x$ versus $y - 1$ along the free surface. We note that the same weakly nonlinear solution is obtained if the pressure distribution is replaced by a triangle of height $h = A^{1/2} = 0.1$ (see (2.16)).

The analysis in the weakly nonlinear phase plane (figure 3*d*) determines the number of independent parameters we need to fix to obtain a unique solution (namely four: F, A, σ_c and x_p). The length of surfboard is given by L and elevation of the free-surface by γ, In the next subsection, we consider subcritical flow, $F < 1$, past an inclined plate.

3.2. *Subcritical flow past pressure distributions and an inclined plate*

Binder & Vanden-Broeck (2005) showed that there are no solutions for subcritical flow ($F < 1$), past a plate, that satisfy the radiation condition. All solutions have trains of waves both far upstream and far downstream (i.e. as $x \to \pm\infty$).

We first introduce a pressure distribution to eliminate the train of waves extending to $x \to \infty$. The flow has then to be reversed to obtain a physically realistic solution (such a reversal was done in figure 4 of this paper.). Figures 4(*a*) and 4(*c*) are nonlinear and weakly nonlinear solutions for a given value of $F = 0.76$. The length L of the

plate and position x_p of the pressure distribution came as part of the solution. If these two parameters are fixed, there are, in general, three trains of waves (one far upstream, one far downstream and one between the two disturbances). We could obtain solutions that satisfy the radiation condition with two trains of waves on the free surface. In figures 4(a) and 4(c), we chose to eliminate two of the trains of waves and to allow one train of waves to remain on the free surface.

The nonlinear and weakly nonlinear profiles (figure 4a, c) are in good agreement for $F = 0.76$. The agreement improves when values of F closer to 1 are chosen. The analysis in the weakly nonlinear phase plane is shown in figure 4(d). The nonlinear phase trajectories in figure 4(b) provide a check that the weakly nonlinear analysis is correct.

We note that qualitatively similar profiles could be obtained by replacing the pressure distribution with a triangle in figures 4(a) and 4(c).

In the next subsection, we consider generalized critical flow, $F > 1$, past a pressure distribution and under an inclined sluice gate.

3.3. *Generalized critical flow past a pressure distribution and under an inclined sluice gate*

Binder & Vanden-Broeck (2005) showed that the only possible flows under an inclined sluice gate are generalized critical flows (i.e. flows with $F > 1$ and a train of waves as $x \to -\infty$). There are therefore no solutions that satisfy the radiation condition. By introducing another disturbance such as pressure distribution, we now show that we can eliminate these waves, thus satisfying the radiation condition.

Figure 5(a) is a computed free-surface profile for flow past a pressure distribution and under an inclined sluice gate for given values of $F = 1.30$, $\sigma_c = 3.4°$, $\gamma = 0.79$ (tangential separation at $x = 0$), $A = 0.01$ and $x_p = -16.44$. The length of the gate $L = 6.92$, came as part of the solution. In general, there are two trains of waves on the upstream free surface and the radiation condition is not satisfied as $x \to -\infty$.

The weakly nonlinear phase plane is obtained by combining the phase portrait of figure 2(a) with a horizontal jump modelling the gate, a vertical jump modelling the distribution of pressure. This is illustrated in figure 5(c) which is a weakly nonlinear phase portrait for figure 5(a). These weakly nonlinear results are in good agreement with the corresponding nonlinear results of figure 5(b).

Now by allowing two of the independent parameters to come as part of the solution (e.g. A and x_p) we can force the free surface to be flat as $x \to -\infty$. Figure 6(a) is a computed nonlinear free-surface profile for a given value $F = 1.30$. We also derived analytically a similar weakly nonlinear profile for, $F = 1.30$, in figure 6(c). The flow in figure 6(a, c) is critical ($F > 1$, $F^* < 1$) and the radiation condition is satisfied as $x \to -\infty$.

So far, we have considered only flows in a channel disturbed by two of our three different types of disturbance (i.e. a gate and a distribution of pressure). We consider in the next subsection the flow past an obstacle on the bottom of the channel and under a vertical sluice gate.

3.4. *Generalized critical flow past a triangle and under a vertical sluice gate*

Vanden-Broeck (1996) considered the flow under a vertical sluice gate. In accordance with the findings of Binder & Vanden-Broeck (2005), he found that there are always waves as $x \to -\infty$. Therefore there are no solutions satisfying the radiation condition. In this subsection, we show how to eliminate the waves as $x \to -\infty$ by introducing a

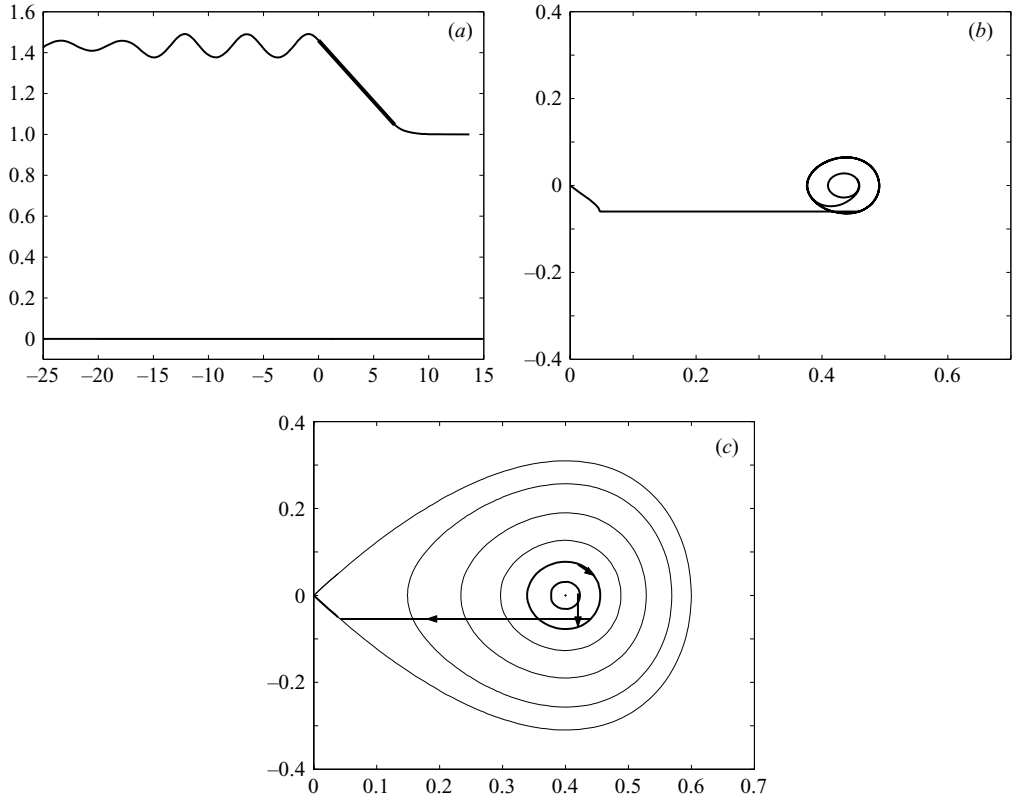

FIGURE 5. Generalized critical flow past a pressure distribution and under an inclined sluice gate. (*a*) Fully nonlinear free-surface profile for values of $F = 1.30$, $L = 6.92$, $\gamma = 0.79$, $\sigma_c = 3.4°$, $A = 0.01$ and $x_p = -16.44$. (*b*) Values of $\mathrm{d}y/\mathrm{d}x = \tan(\theta)$ versus $y - 1 = \eta$, showing the fully nonlinear phase trajectories for (*a*). (*c*) Weakly nonlinear phase portrait for (*a*), $\mathrm{d}\eta/\mathrm{d}x$ versus η.

second disturbance. We choose this disturbance to be the submerged obstacle since results with the pressure distribution have already been described in the previous subsection.

Figure 7(*a*) is a profile for the flow past a triangle on the bottom of the channel and under a vertical sluice gate for given values of $\sigma_c = 90°$, $\gamma = 1.00$ (stagnation point at the separation point B), $L = 1.00$, $\sigma_t = 45°$, $h = 0.55$ and $x_t = -11.53$. The downstream Froude number $F = 1.84$ came as part of the solution. In general, there are two trains of waves of different amplitude on the upstream free surface for the flow past a submerged obstacle and a vertical sluice gate (see figure 7*a*). The radiation condition is not satisfied far upstream as $x \to -\infty$.

By allowing the triangles height h and position x_t to come as part of the solution and forcing the free surface flat as $x \to -\infty$, the waves can be eliminated far upstream and the radiation condition is then satisfied. We moved the triangle along the bottom of the channel, closer to sluice gate in figure 7(*b*), before allowing h and x_t to come as part of the solution. This allowed us to eliminate all the waves appearing on the free surface.

We also found that the shape or geometry of the disturbance on the bottom of the channel did not affect qualitatively the solutions. This is illustrated in figures 7(*b*), 7(*c*) and 7(*d*) for different values of σ_t, h and x_t.

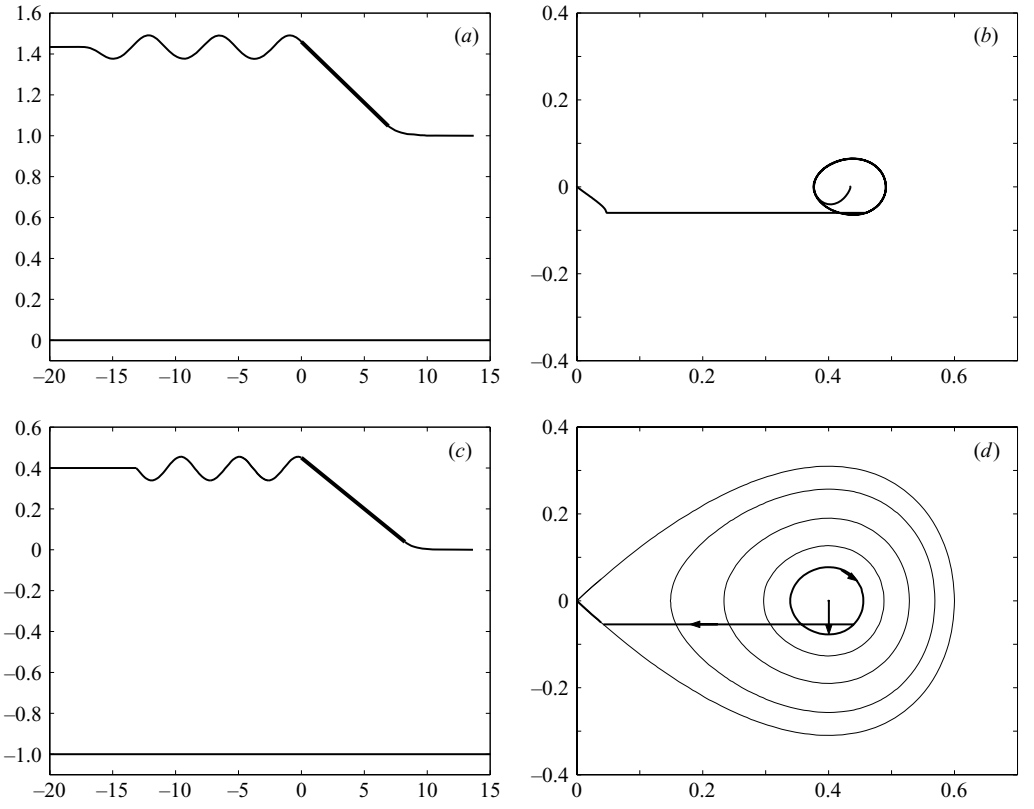

FIGURE 6. Critical flow past a pressure distribution and under an inclined sluice gate. (*a*) Fully nonlinear free-surface profile for values of $F = 1.30$, $L = 6.92$, $\gamma = 0.79$, $\sigma_c = 3.4°$, $A = 0.02$ and $x_p = -16.41$. (*b*) Values of $\mathrm{d}y/\mathrm{d}x = \tan(\theta)$ versus $y - 1 = \eta$, showing the fully nonlinear phase trajectories for (*a*). (*c*) Weakly nonlinear free surface profile for values of $F = 1.30$, $L = 8.23$, $\gamma = 0.79$, $\sigma_c = 2.9°$, $A = 0.02$ and $x_p = -13.13$. (*d*) Weakly nonlinear phase portrait for (*c*), $\mathrm{d}\eta/\mathrm{d}x$ versus η.

The weakly nonlinear theory assumes that the slope of the streamline $ABCD$ in figure 1(*a*) is small. Therefore, the weakly nonlinear theory cannot be used to model the flow under a vertical sluice gate and no comparisons with weakly nonlinear results can made in this subsection.

In the next subsection we consider flow in a channel past all three types of disturbance.

3.5. *Generalized critical free-surface flows with multiple disturbances in a channel*

In this section, we discuss results with all three types of disturbance (sluice gate, pressure distribution and triangle) included. To illustrate that the results are qualitatively independent of the precise form of the distribution of pressure, we present results for a different pressure distribution from the one defined by (2.9), namely

$$\left.\begin{array}{ll} P = A\mathrm{e}^{[1/[(x-x_p)^2-\beta_p^2]]} & \text{for} \quad x_p - \beta_p < x < x_p + \beta_p, \\ P = 0 & \text{otherwise.} \end{array}\right\} \tag{3.1}$$

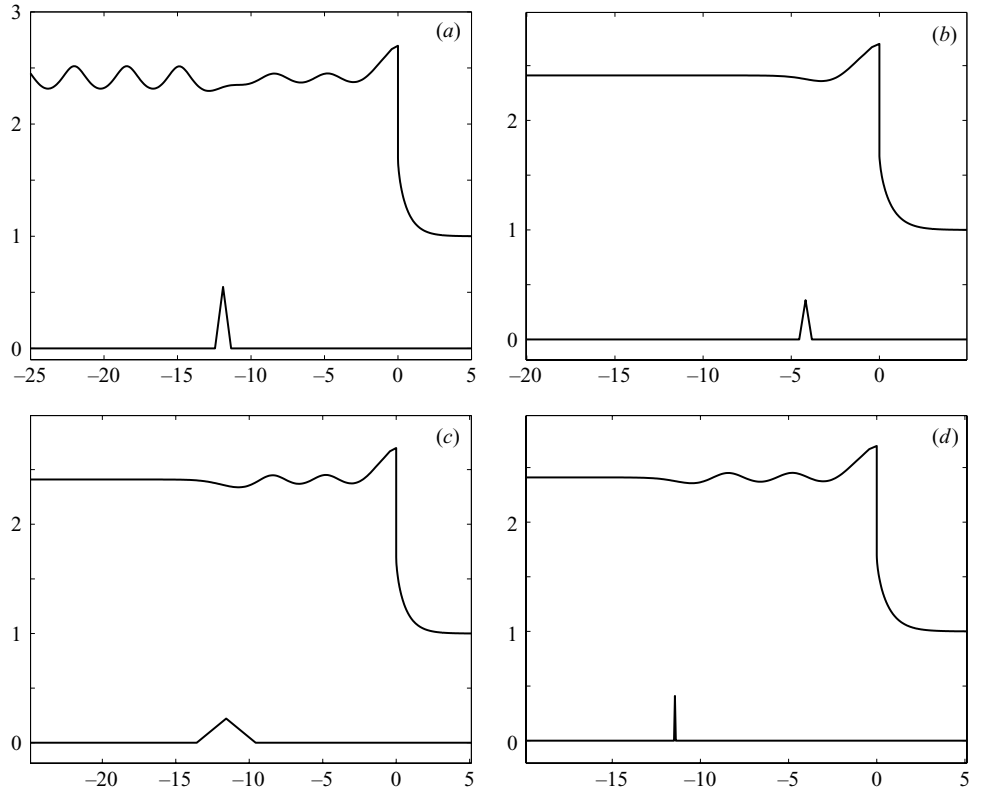

FIGURE 7. Generalized critical flow and critical flow past a disturbance on the bottom of a channel and under a vertical sluice gate for the values of $F = 1.84$, $\gamma = 1.00$, $\sigma_c = 90°$ and $L = 1.00$. (*a*) The values for the triangle are $h = 0.55$, $x_t = -11.53$ and $\sigma_t = 45°$. (*b*) The values for the triangle are $h = 0.36$, $x_t = -4.18$ and $\sigma_t = 45°$. (*c*) The values for the triangle are $h = 0.22$, $x_t = -11.57$ and $\sigma_t = 6.3°$. (*d*) The values for the triangle are $h = 0.41$, $x_t = -11.45$ and $\sigma_t = 82.8°$.

We first discuss solutions for an inclined sluice gate, a triangle and a pressure distribution upstream of the gate. In general, there are three trains of waves on the upstream free surface and a uniform supercritical stream as $x \to \infty$. Two of the trains of waves are 'trapped' between the disturbances (pressure distribution, obstacle and gate) and one train of waves extends far upstream. Figure 8(*a*) is a computed profile. The downstream Froude number $F = 1.87$ came as part of the solution. We note that the radiation condition is not satisfied since there is a train of waves as $x \to -\infty$.

Since the flow separates tangentially from the sluice gate at $x = 0$ ($\gamma = 0.95$) in figure 8(*a*), we can analyse the solution in the weakly nonlinear phase space (see figure 8*b*). The vertical and horizontal lines in figure 8(*b*) correspond to the triangle or pressure disturbances and inclined sluice gate, respectively. The bold inner periodic orbits in figure 8(*b*) correspond to the three trains of waves in figure 8(*a*). We are outside the expected range of validity of the weakly nonlinear analysis since F is not close to 1. However, the agreement between nonlinear and weakly nonlinear theories is still good.

Following the analysis of the flow past two disturbances of figure 6(*a*), we can eliminate the train of waves that appears upstream of the last disturbance on the free

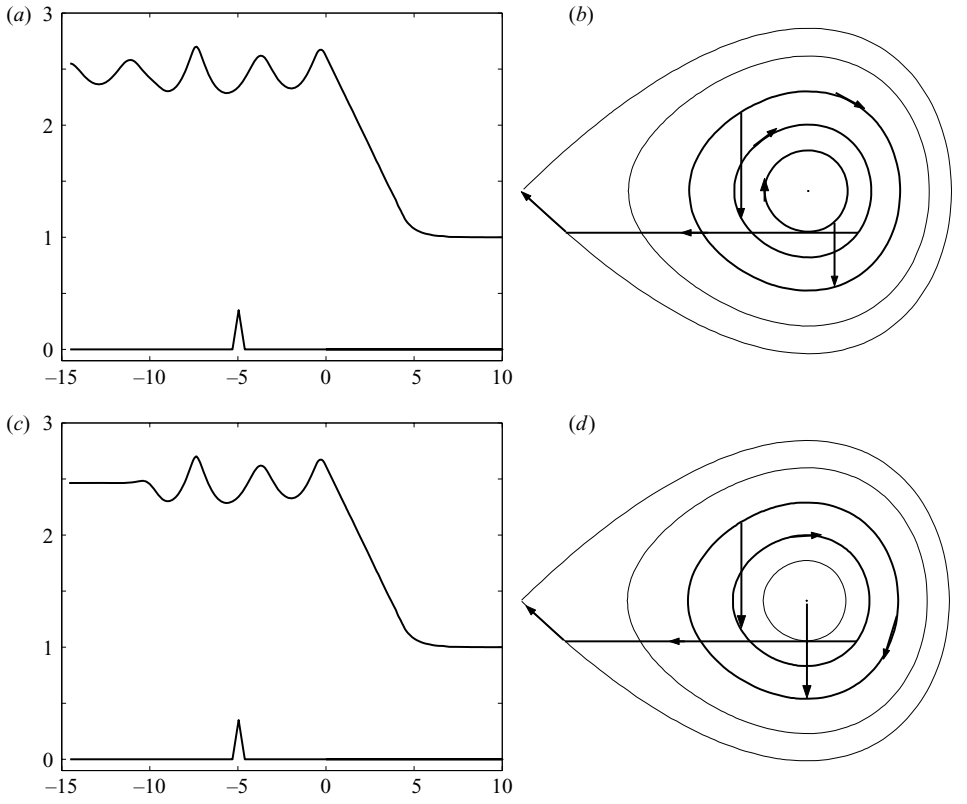

FIGURE 8. Generalized critical flow and critical flow past a pressure distribution, triangle and inclined sluice gate. (*a*) The values for the Froude number and gate are, $F = 1.87$, $L = 4.65$, $\gamma = 0.95$ and $\sigma_c = 18°$. The values for the pressure distribution are, $x_p = -9.63$, $A = 3.50$ and $\beta_p = 0.45$. The values for the triangle are $h = 0.35$, $x_t = -4.97$ and $\sigma_t = 45°$. (*b*) Sketch of the weakly nonlinear phase portrait for (*a*). (*c*) The values for the Froude number and gate are, $F = 1.87$, $L = 4.65$, $\gamma = 0.95$ and $\sigma_c = 18°$. The values for the pressure distribution are, $x_p = -9.90$, $A = 3.50$ and $\beta_p = 0.49$. The values for the triangle are $h = 0.35$, $x_t = -4.96$ and $\sigma_t = 45°$. (*d*) Sketch of the weakly nonlinear phase portrait for (*c*).

surface. Figure 8(*c*) is a computed profile for $F = 1.87$ and the radiation condition is now satisfied as $x \to -\infty$. Figure 8(*d*) illustrates the analysis in the phase plane for the solution of figure 8(*c*).

We can also construct solutions where the disturbances are a pressure distribution a triangle and a vertical sluice gate (see figures 1*a* and 9*a*, *b*). In general, these solutions have three trains of waves and do not satisfy the radiation condition far upstream (see figure 1*a*). By allowing two of the given parameters to come as part of the solution, one of the trains of waves can be eliminated.

In figure 9(*a*), we have eliminated the waves between two of the disturbances (pressure distribution and triangle). The solution lacks physical meaning in figure 9(*a*) as the radiation condition is not satisfied as $x \to -\infty$. However, by introducing another disturbance upstream of the last disturbance (pressure) in figure 9(*a*), we could eliminate the waves as $x \to -\infty$. In figure 9(*b*), the waves have been eliminated far upstream and the radiation condition is satisfied.

Another qualitatively different type of solution is shown in figures 9(*c*) and 9(*d*).

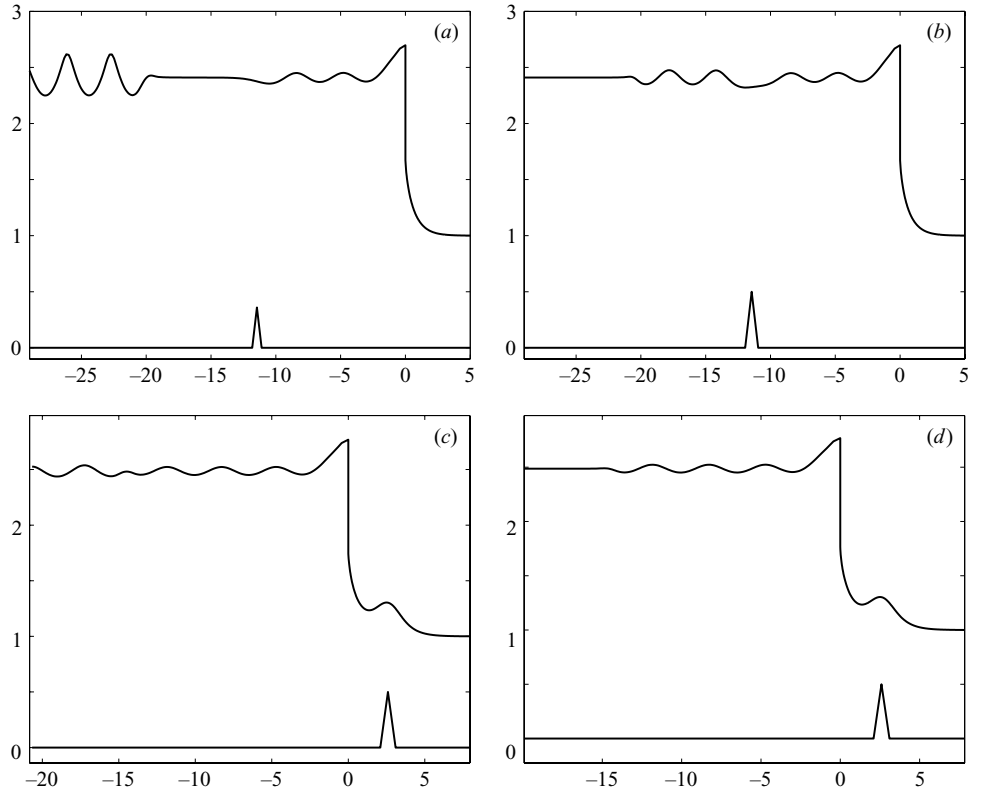

FIGURE 9. Generalized critical flow and critical flow past a pressure distribution, triangle and vertical sluice gate. The values for the gate are $L = 1.00$, $\gamma = 1.00$ and $\sigma_c = 90°$. (*a*) The values for the Froude number and pressure distribution are, $F = 1.84$, $x_p = -20.11$, $A = 3.39$ and $\beta_p = 0.50$. The values for the triangle are $h = 0.36$, $x_t = -11.54$ and $\sigma_t = 45°$. (*b*) The values for the Froude number and pressure distribution are, $F = 1.84$, $x_p = -20.58$, $A = 6.09$ and $\beta_p = 0.43$. The values for the triangle are $h = 0.50$, $x_t = -11.45$ and $\sigma_t = 45°$. (*c*) The values for the Froude number and pressure distribution are, $F = 1.88$, $x_p = -14.55$, $A = 2.47$ and $\beta_p = 0.48$. The values for the triangle are $h = 0.50$, $x_t = 2.59$ and $\sigma_t = 45°$. (*d*) The values for the Froude number and pressure distribution are, $F = 1.88$, $x_p = -14.47$, $A = 1.76$ and $\beta_p = 0.46$. The values for the triangle are $h = 0.50$, $x_t = 2.59$ and $\sigma_t = 45°$.

4. Conclusion

In previous work, fully nonlinear numerical solutions and analytical weakly nonlinear solutions were obtained for free-surface flows under a sluice gate or past a plate in a channel. It was found that there were no subcritical flows or critical flows satisfying the radiation condition. In both cases, there were trains of waves which did not satisfy the radiation condition. In this paper, we showed that these unphysical waves can be eliminated by introducing further disturbances in the flow. In addition, new families of free-surface flows past multiple disturbances were identified and studied.

REFERENCES

ASAVANANT, J. & VANDEN-BROECK, J.-M. 1994 Free-surface flows past a surface-piercing object of finite length. *J. Fluid. Mech.* **273**, 109–124.

Asavanant, J. & Vanden-Broeck, J.-M. 1996 Nonlinear free-surface flows emerging from vessels and flows under a sluice gate. *J. Austcal. Math. Soc.* **38**, 63–86.

Benjamin, T. B. 1956 On the flow in channels when rigid obstacles are placed in the stream. *J. Fluid Mech.* **1**, 227–248.

Binder, B. J. & Vanden-Broeck, J.-M. 2005 Free surface flows past surfboards and sluice gates. *Eur. J. Appl. Maths* **16**, 601–619.

Binder, B. J., Dias, F. & Vanden-Broeck, J.-M. 2005 Forced solitary waves and fronts past submerged obstacles. *Chaos* **15**, 037106.

Binnie, A. M. 1952 The flow of water under a sluice gate.

Chung, Y. K. 1972 Solution of flow under a sluice gates. *ASCE J. Engng Mech. Div.* **98**, 121–140.

Dias, F. & Vanden-Broeck, J.-M. 1989 Open channel flows with submerged obstructions. *J. Fluid Mech.* **206**, 155–170.

Dias, F. & Vanden-Broeck, J.-M. 2002 Generalized critical free-surface flows. *J. Engng Maths* **42**, 291–301.

Dias, F. & Vanden-Broeck, J.-M. 2004 Trapped waves between submerged obstacles. *J. Fluid Mech.* **509**, 93–102.

Forbes, L.-K. 1981 On the resistance of a submerged semi-elliptical body. *J. Engng Maths* **15**, 287–298.

Forbes, L.-K. 1988 Critical free-surface flow over a semi-circular obstruction. *J. Engng Maths* **22**, 3–13.

Forbes, L.-K. & Schwartz, L. W. 1982 Free-surface flow over a semicircular obstruction. *J. Fluid Mech.* **114**, 299–314.

Frangmeier, D. D. & Strelkoff, T. S. 1968 Solution for gravity flow under a sluice gate. *ASCE J. Engng Mech. Div.* **94**, 153–176.

Lamb, H. 1945 *Hydrodynamics*, 6th edn, chap. 9. Dover.

Larock, B. E. 1969 Gravity-affected flow from planar sluice gate. *ASCE J. Engng Mech. Div.* **96**, 1211–1226.

Shen, S. S.-P. 1995 On the accuracy of the stationary forced Korteweg–de Vries equation as a model equation for flows over a bump. *Q. Appl. Maths* **53**, 701–719.

Vanden-Broeck, J.-M. 1987 Free-surface flow over an obstruction in a channel. *Phys. Fluids* **30**, 2315–2317.

Vanden-Broeck, J.-M. 1996 Numerical calculations of the free-surface flow under a sluice gate. *J. Fluid Mech.* **330**, 339–347.

Vanden-Broeck, J.-M. & Keller, J. B. 1989 Surfing on solitary waves. *J. Fluid Mech.* **198**, 115–125.